Charge Mobility of Discotic Mesophases: A Multiscale Quantum and Classical Study

James Kirkpatrick,[1] Valentina Marcon,[2] Jenny Nelson,[1] Kurt Kremer,[2] and Denis Andrienko[2]

[1]*Department of Physics, Imperial College London, Prince Consort Road, London SW7 2BW, United Kingdom*
[2]*Max-Planck-Institut für Polymerforschung, Ackermannweg 10, 55128 Mainz, Germany*

A correlation is established between the molecular structure and charge mobility of discotic mesophases of hexabenzocoronene derivatives by combining electronic structure calculations, molecular dynamics, and kinetic Monte Carlo simulations. It is demonstrated that this multiscale approach can provide an accurate *ab initio* description of charge transport in organic materials.

Graphene and graphenelike molecules have attracted considerable interest in the past years due to their unusual electronic properties [1], self-assembly [2], and role in the evolutionary scheme of the Universe [3]. Their recent application in organic photovoltaic (OPV) devices [4] relies upon blend films combining a large interfacial area for charge separation and recombination with efficient vertical transport paths. Transport in organic electronic materials proceeds by incoherent hopping and depends upon both local molecular ordering and macroscopic percolation paths. Improved mobilities, which are crucial to improved OPV device performance, thus require control of structure on both the molecular and macroscopic length scales.

Thermotropic discotic liquid crystals could be ideal for OPV as they offer optimal design possibilities for both the charge mobility and the necessary underlying mesoscopic morphology. They are formed by flat molecules with a central aromatic core and aliphatic side chains [5]. In the columnar phase the molecules stack on top of each other into columns and then arrange in a regular lattice. Along the stacks of aromatic cores in the column one-dimensional charge transport is observed [4,6]. Perpendicular to the column axis the charges have to tunnel through the insulating side chains, resulting in a much reduced mobility. Columnar mesophases can laterally segregate into phases of donor and acceptor molecules providing high interface areas and efficient percolation pathways. The reported high charge mobilities [6] would guarantee efficient operation. However, the spatial arrangement of stacks is never perfect: the columns can be misaligned, tilted, or form various types of topological defects. Both the local alignment of the molecules in columns and the global arrangement of the columns in the mesophase are sensitive to molecular architecture, such as the type of attached side chains [7].

A key question is the influence of local order in discotic mesophases on charge transport. However, the task is challenging because different theoretical methods are needed to describe different length- and time-scale phenomena. Atomistic simulations are needed for local molecular arrangements [7], quantum chemical calculations for the electron transfer mechanisms and interaction with the electrodes [8], and stochastic or rate-equation dynamic methods for simulation of charge dynamics.

In this Letter, we present the first statistical mechanics evaluation of charge mobility based on quantum chemical and atomistic molecular dynamics (MD) methods, and we link the results to the microscopic structure of columns. We employ such a three level approach to explain the side chain dependence of charge mobility for differently substituted hexabenzocoronene (HBC) derivatives.

Previous studies of liquid crystalline (LC) triphenylene derivatives [9] suggest that thermally activated hopping is an appropriate description of microscopic charge transport in these materials. This is also supported by studies on LCs with different cores, where changes in mobility can be rationalized in terms of the different internal reorganization energies [10], a typical signature of small polaron hopping. For this reason we use the Marcus-Hush formalism [11] for the charge transfer rate ω_{ij}

$$\omega_{ij} = \frac{|J_{ij}|^2}{\hbar}\sqrt{\frac{\pi}{\lambda kT}}\exp\left[-\frac{(\Delta G_{ij} - \lambda)^2}{4\lambda kT}\right], \qquad (1)$$

J_{ij} is the transfer integral for electron or hole transfer, ΔG_{ij} the difference in free energy between the initial and final states, λ the reorganization energy, $\hbar$ Planck's constant, k Boltzmann's constant, and T the temperature. J_{ij} and λ can be computed using quantum chemical methods [8]. J_{ij} is highly sensitive to the relative position and orientation of the molecules involved, which will be determined, in turn, using MD. We include only the electric field $\boldsymbol{F}$ in the evaluation of the free energy and write $\Delta G_{ij} = \boldsymbol{F} \cdot \boldsymbol{d}_{ij}$, where $\boldsymbol{d}_{ij}$ is the displacement between molecules. We neglect variations in site energy due to disorder in electrostatic interactions between the molecules, because such differences vanish when the conjugated cores are parallel. Furthermore, the exclusion of site energy disorder allows us to focus exclusively on the effect of configurational disorder on charge transport through disorder induced variations in J_{ij}.

Once all ω_{ij} are known, charge dynamics can be computed, by simulation or approximate methods. Though
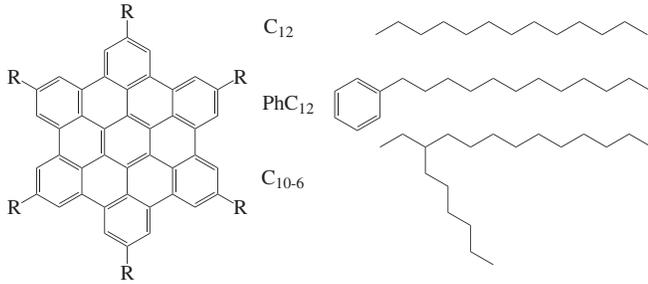
FIG. 1. Stick diagram of HBC derivatives with different side chains. We studied alkyl chains of different lengths, C_n, with $n = 10, 12, 14, 16$, branched side chains, C_{10-6}, and the dodecylphenyl-substituted side chains PhC_{12}.

several aspects of the problem are treated in the literature [10,12,13], a comprehensive study on large columnar systems does not yet exist. Here we use a combination of methods to achieve a truly *ab initio* description of charge mobility in HBC: (i) MD simulations are performed on discotic mesophases of different HBC derivatives, (ii) the obtained molecular positions and orientations are used to calculate the transfer integral J for all neighboring pairs of molecules in a column, and (iii) charge dynamics are determined using kinetic Monte Carlo (MC) methods [14].

All studied HBC derivatives are given in Fig. 1. The molecules consist of a flat aromatic core and six side chains. Experimental data on their structural properties [6,15–18], as well as pulse radiolysis time resolved microwave conductivity (PR-TRMC) data, [6,19] are available.

Details of the force field and the MD setup can be found in Ref. [7]. The molecules were arranged in 16 columns with 10 molecules in a column. Production runs of 100 ns were performed at constant pressure of 0.1 MPa and temperature $T = 300$ K fixed using the Berendsen method with anisotropic pressure coupling. In total, 200 snapshots were saved for each run. For each MD snapshot, the overlap integrals J_{ij} between intracolumnar nearest neighbors i and j were calculated. To calculate J_{ij}, the aromatic core of each molecule, as output by the MD simulation, is replaced by a rigid copy of the energy minimized configuration, with the same axial and torsional orientation. Because of molecular symmetry, the highest occupied molecular orbital (HOMO) and the lowest unoccupied molecular orbital (LUMO) of HBC are doubly occupied. Thus we have to calculate four transfer integrals for hole and four for electron transport [12]. For each component we used an adaptation of the Zerner's intermediate neglect of differential overlap (ZINDO) method [20]. The effective J values are then taken as the root-mean square of the four HOMO transfer integrals for holes and of the four LUMO transfer integrals for electrons [21]. The inner-sphere reorganization energy for cation and anion radicals was calculated using unrestricted wave functions, the Becke three-parameter Lee-Yang-Parr (B3LYP) hybrid functional, and 6-31G(d,p) basis set. We found reorganization energies λ

of 0.13 eV for cations and 0.11 eV for anions in agreement with Ref. [10]. The outer-sphere contribution was neglected.

For kinetic MC, columns of molecules produced by MD are stacked periodically to produce a stack 1 μm thick. A uniform field is applied along the stack, a charge carrier representing either an electron or a hole is introduced near one end, and the charge drift is simulated by a continuous-time random walk algorithm, similar to Ref. [22] with adjustments for a disordered lattice. Simulated transients are averaged over many different starting positions of the charge and many realizations of the lattice from the MD snapshots. This sampling method is analogous to the experimental situation where charges are generated in parallel columns of different configuration, and the measured transient is the sum of displacement currents from all columns. The charge mobility μ is obtained from the transit time t_{Tr} of the simulated transient via $\mu = L/Ft_{Tr}$, where L is the stack thickness. t_{Tr} is taken as the point of intersection of the two asymptotes to the simulated photocurrent plotted on a log-log plot, as would be done in a time-of-flight (TOF) experiment.

The results of TOF simulations are shown in Fig. 2(a). Comparison at the same F shows that the C_{10-6} structures lead to relatively dispersive transients while those for C_{10}-C_{16} lead to the nondispersive transients typical of ordered materials [23]. In our approach, where energetic disorder is neglected, disorder in charge transport can only arise from fluctuations in the nearest-neighbor transfer integrals J, which in turn arise from disorder in intermolecular separation and orientation.

The distributions of the transfer integrals, $\log|J|^2$, are shown in Fig. 2(b): C_{12} has a very narrow distribution, PhC_{12} is wider and shifted to smaller values of J, while C_{10-6} is shifted to higher values and has a second peak at low values of J. There are several microscopic factors which can affect these distributions: the intermolecular distance, the relative molecular tilt and rotation, and the lateral displacement of molecules with respect to each other. In order to relate variation in transit times (i.e., mobilities) to the microscopic structure, we present the distributions of intermolecular distances, g_z, in Fig. 2(c). g_z shows that the molecular alignment of C_{12} is almost perfect (it has a set of narrow peaks separated by 0.37 nm); C_{10-6} and PhC_{12} have much wider peaks, and the peaks of PhC_{12} are shifted due to the larger average intermolecular distance. These observations partially explain the differences between the distributions of the transfer integrals, i.e., the broadening for C_{10-6} and PhC_{12} compared to C_{12} and the shift of the peak for PhC_{12} to smaller values of J.

However, g_z does not explain either the shift of the peak of the $|J|^2$ distribution for C_{10-6} to higher values (the intermolecular distance does not change compared to C_{12}) or the presence of the second peak, at low J, in this distribution. Detailed analysis of the MD snapshots shows
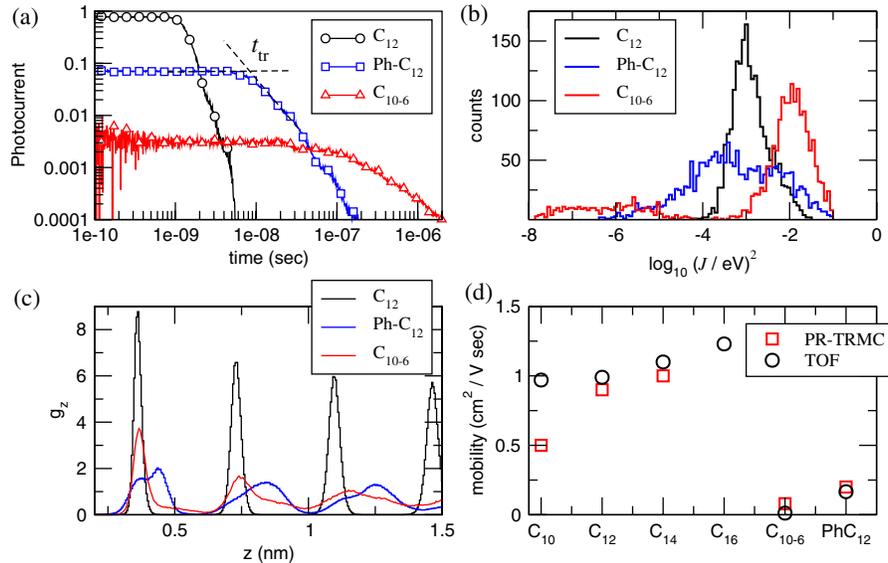
FIG. 2 (color online).   (a) Simulated TOF hole photocurrent transients for C_{12}, PhC_{12}, and C_{10-6} at $T = 300$ K and $F = 10^5$ V cm^{-1}. Traces are averaged over 200 snapshots with columns of length 10. (b) Frequency plots of the logarithm of the transfer integral squared. In each case, results for C_{10}-C_{16} are practically indistinguishable from C_{12} on the scales used. (c) Intracolumnar radial distribution function g_z (normalized probability of two molecules in the same column to be separated by the distance z from each other). (d) Sum of simulated electron and hole mobilities in comparison with experimental values (PR-TRMC).

that the increase of the modal transfer integral for C_{10-6} is due to good azimuthal registration for branched side chains which minimizes relative rotations so that the transfer integral is maximal. The second peak in the distribution is due to defects in the columnar molecular arrangement: in case of C_{10-6} the columns comprise well-aligned subcolumns (4−5 molecules each) which, however, are slightly misaligned with respect to each other. This can be seen from the representative MD snapshots of two of the systems in Fig. 3. The absence of well-resolved higher-order peaks in g_z is also an indirect indication of the presence of these defects. Thus, the low J peak represents bottlenecks at discontinuities in the stacks, which act as traps in the one-dimensional transport paths, leading to comparatively small values of charge mobilities. In this sense, one-dimensional ordering makes these materials extremely susceptible to defects. The analysis of the microscopic morphology implies that charge transport is sensitive not only to changes of the standard order parameters, such as the nematic order parameter and the mean and half-width of distributions, but to the entire positional and orientational distribution functions of molecules, and, in particular, to the low $|J|^2$ values.

Finally, we compare our simulations to PR-TRMC measurements. PR-TRMC probes the sum of high frequency photoinduced conductivities due to both types of charge carriers. It therefore probes the fastest contributions to charge transport and is sensitive only to local disorder within well-ordered domains. PR-TRMC mobilities are therefore appropriate for comparison with our simulation since the column sizes we are using are small. TOF mo-

bility data would, in contrast, be heavily dependent on defects and on fluctuations with wavelengths longer than the column size we have used, while to simulate TOF experiments for practical film thicknesses, large systems should be studied, which would require a multiscale ansatz [24].

The simulated mobilities are compared with experimental data in Table I and in Fig. 2(d). The good agreement for both the C_{10}-C_{16} series (where differences in mobility are small) and for the PhC_{12} and C_{10-6} derivatives (which have much smaller mobilities) suggests that our procedure and the morphologies are appropriate. Of particular interest is the strong sensitivity of μ to the degree of order in the columns, which is itself controlled by the side chain type as shown in the present study.

In summary, three methods were combined into one scheme to determine the charge mobilities: (i) quantum chemical methods for the calculation of molecular electronic structures and reorganization energies, (ii) molecular dynamics for simulation of the relative
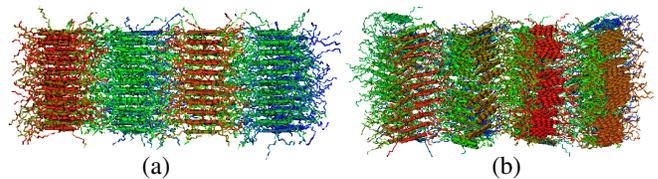

FIG. 3 (color online).   MD simulation snapshots of columns of 10 HBC molecules with (a) C_{12} and (b) C_{10-6} side chains at 300 K. Columns are prearranged on a rectangular lattice.

TABLE I. Electron (*e*) and hole (*h*) mobilities ($cm^2\,V^{-1}\,s^{-1}$) of different compounds calculated using the multiscale model method in comparison with experimentally measured PR-TRMC mobilities. Also shown are the nematic order parameter S and the average vertical separation between cores of HBC molecules h (nm).

Compound	$\mu_{PR\text{-}TRMC}$	μ_{sim}^e	μ_{sim}^h	S	h
C_{10}	0.5 [6]	0.22	0.75	0.98	0.36
C_{12}	0.9 [6]	0.23	0.76	0.98	0.36
C_{14}	1 [6]	0.27	0.80	0.98	0.36
C_{16}	—	0.29	0.91	0.98	0.36
C_{10-6}	0.08 [19]	—	0.01	0.96	0.36
PhC_{12}	0.2 [6]	0.036	0.13	0.95	0.44

positions and orientations of molecules in a columnar mesophase, and (iii) kinetic Monte Carlo simulations to simulate charge transport. Applying this scheme to differently substituted HBC derivatives, we reproduce the trends and magnitudes of mobilities as measured by PR-TRMC and connect mobility directly to the microscopic morphology of the columns. Most other studies of charge transport are based on the use of arbitrary distributions in the microscopic rate-controlling parameters [14,25]. These methods are certainly capable of describing one of our results, namely, that in one-dimensional transport charge traps are rate limiting. However, returning to the example of the C_{10-6} system, we find that mobility is defined by a double peaked distribution in transfer integrals: such a distribution has never before been proposed in an empirical charge transport model. Our study also shows that it is possible to understand and reproduce experimental charge transport parameters, and, in principle, accurately predict them. For example, designing side chains with a favorable core rotation, as for C_{10-6}, but without the tendency for columnar defects would improve mobilities significantly.

[1] K. S. Novoselov, A. K. Geim, S. V. Morozov, D. Jiang, M. I. Katsnelson, I. Grigorieva, S. V. Dubonos, and A. Firsov, Nature (London) **438**, 197 (2005).
[2] F. Hoeben, P. Jonkheijm, E. Meijer, and A. Schenning, Chem. Rev. **105**, 1491 (2005).
[3] T. Henning and F. Salama, Science **282**, 2204 (1998).
[4] L. Schmidt-Mende, A. Fechtenkotter, K. Mullen, E. Moons, R. H. Friend, and J. D. MacKenzie, Science **293**, 1119 (2001).
[5] S. Chandrasekhar and G. S. Ranganath, Rep. Prog. Phys. **53**, 57 (1990).
[6] A. M. van de Craats, J. M. Warman, A. Fechtenkotter, J. D. Brand, M. A. Harbison, and K. Müllen, Adv. Mater. **11**, 1469 (1999).
[7] D. Andrienko, V. Marcon, and K. Kremer, J. Chem. Phys. **125**, 124902 (2006).
[8] J. L. Bredas, D. Beljonne, V. Coropceanu, and J. Cornil, Chem. Rev. **104**, 4971 (2004).
[9] T. Kreouzis, K. Donovan, N. Boden, R. Bushby, O. Lozman, and Q. Liu, J. Chem. Phys. **114**, 1797 (2001).
[10] V. Lemaur, D. Da Silva Filho, V. Coropceanu, M. Lehmann, Y. Geerts, J. Piris, M. Debije, A. Van de Craats, K. Senthilkumar, and L. Siebbeles *et al.*, J. Am. Chem. Soc. **126**, 3271 (2004).
[11] K. F. Freed and J. Jortner, J. Chem. Phys. **52**, 6272 (1970).
[12] K. Senthilkumar, F. Grozema, F. Bickelhaupt, and L. Siebbeles, J. Chem. Phys. **119**, 9809 (2003).
[13] W. Deng and W. Goddard, J. Phys. Chem. B **108**, 8614 (2004).
[14] P. Borsenberger, L. Pautmeier, and H. Bassler, J. Chem. Phys. **94**, 5447 (1991).
[15] I. Fischbach, T. Pakula, P. Minkin, A. Fechtenkotter, K. Müllen, H. W. Spiess, and K. Saalwachter, J. Phys. Chem. B **106**, 6408 (2002).
[16] A. Fechtenkotter, K. Saalwachter, M. A. Harbison, K. Müllen, and H. W. Spiess, Angew. Chem. **38**, 3039 (1999).
[17] S. P. Brown, I. Schnell, J. D. Brand, K. Müllen, and H. W. Spiess, J. Am. Chem. Soc. **121**, 6712 (1999).
[18] P. Herwig, C. W. Kayser, K. Müllen, and H. W. Spiess, Adv. Mater. **8**, 510 (1996).
[19] W. Pisula, M. Kastler, D. Wasserfallen, M. Mondeshki, J. Piris, I. Schnell, and K. Müllen, Chem. Mat. **18**, 3634 (2006).
[20] J. Kirkpatrick, Int. J. Quant. Chem. (to be published).
[21] M. Newton, Chem. Rev. **91**, 767 (1991).
[22] A. J. Chatten, S. M. Tuladhar, S. A. Choulis, D. D. C. Bradley, and J. Nelson, J. Mater. Sci. Technol. (Sofia) **40**, 1393 (2005).
[23] T. Kreouzis, D. Poplavskyy, S. M. Tuladhar, M. Campoy-Quiles, J. Nelson, A. J. Campbell, and D. D. C. Bradley, Phys. Rev. B **73**, 235201 (2006).
[24] B. Hess, S. Leon, N. van der Vegt, and K. Kremer, Soft Matter **2**, 409 (2006).
[25] S. V. Novikov, D. H. Dunlap, V. M. Kenkre, P. E. Parris, and A. V. Vannikov, Phys. Rev. Lett. **81**, 4472 (1998).